ARTICLES
PUBLISHED ONLINE: 14 FEBRUARY 2010 | DOI: 10.1038/NPHYS1516
nature physics

Analog information processing at the quantum limit with a Josephson ring modulator

N. Bergeal[1], R. Vijay[1,2], V. E. Manucharyan[1], I. Siddiqi[2], R. J. Schoelkopf[1], S. M. Girvin[1] and M. H. Devoret[1]*

Amplifiers are crucial in every experiment carrying out a very sensitive measurement. However, they always degrade the information by adding noise. Quantum mechanics puts a limit on how small this degradation can be. Theoretically, the minimum noise energy added by a phase-preserving amplifier to the signal it processes amounts at least to half a photon at the signal frequency. Here we propose a practical microwave device that can fulfil the minimal requirements to reach the quantum limit. The availability of such a device is of importance for the readout of solid-state qubits, and more generally for the measurement of very weak signals in various areas of science. We discuss how this device can be the basic building block for a variety of practical applications, such as amplification, noiseless frequency conversion, dynamic cooling and production of entangled signal pairs.

The concept of quantum-limited amplification was introduced in the 1950s with the development of the first maser amplifiers[1]. Later, following the work of Haus and Mullen[2], Caves[3] reviewed the subject and introduced a general formalism, which includes all linear amplifiers (that is, an amplifier whose output signal is linearly related to its input signal). His analysis led to a fundamental theorem: a phase-preserving amplifier has to add a minimum amount of noise to the signal it processes. The limit is commonly expressed in terms of the minimal temperature of the noise added (T_N^{added}) by an amplifier to the signal

$$T_N^{added} = \frac{1}{2}\frac{\hbar\omega_S}{k_B} \quad (1)$$

where ω_S is the angular frequency of the signal and k_B is the Boltzmann constant. This corresponds to half a photon added to each signal mode at the input of the amplifier. On the other hand, a phase-sensitive amplifier, in which one quadrature is amplified and the other is de-amplified, is subjected to only a lower limit on the product of the noise added to the two quadratures and can squeeze the quantum noise on one quadrature at the expense of extra noise on the other one. Although such amplifiers can look rather appealing because of their ability to operate potentially below the quantum limit equation (1), they are awkward to use in a wide range of applications, where both the phase and amplitude of the signal carry the information. On the other hand, the so-called non-degenerate parametric amplifier, that is, an amplifier in which a nonlinear system[4,5] with two resonant frequencies is pumped with an oscillatory source, has repeatedly been suggested to be a good candidate as a phase-preserving amplifier reaching the quantum limit[6,7]. It operates with two spatially distinct modes, conventionally called the 'signal' at frequency ω_S and the 'idler' (also known as the 'image') at frequency ω_I. These two modes are coupled in the nonlinear system through the 'pump' at frequency Ω. The device operates as an amplifier with photon-number gain when $\Omega = \omega_S + \omega_I$ or as a frequency converter without photon-number gain when $\Omega = |\omega_S - \omega_I|$ (refs 4, 5).

In this article, we shall focus on the phase-preserving case and show that a practical, non-degenerate parametric amplifier operating in the microwave domain can be realized with a simple circuit involving Josephson tunnel junctions. Because it is minimal in the number of active modes, it should reach the quantum limit. Unlike microwave superconducting quantum interference devices, which are powered by a d.c. bias and operate with incoherent Josephson radiation[8,9], Josephson parametric amplifiers involve a coherent microwave source. Josephson-tunnel-junction parametric amplifiers have so far mainly focused on degenerate amplifiers ($\omega_S = \omega_I$), which operate as phase-sensitive amplifiers[10–12], and very little work has been devoted to phase-preserving amplifiers. The difficulty of building a practical device matching the theoretical proposals as well as the lack of applications requiring quantum-limited performances have contributed to put this field on hold. However, recent progress in quantum information processing using microwave interrogation of solid-state qubits[13–16] gave rise to a growing need for low-noise amplifiers that are sensitive enough to measure the extremely weak signals involved in these new devices and renewed the interest in parametric amplifiers[17–20]. Also, amplifiers operating near the quantum limit are essential in quantum feedback for sustaining the coherent oscillation of a qubit[21,22].

The Josephson ring modulator

Even at zero temperature, internal dissipation in a device inevitably adds noise to the output signals. Thus, it is important to build a completely dissipationless circuit using only dispersive elements. The amplifier that we describe here is based on a particularly interesting unusual nonlinear device, which we call the Josephson ring modulator, by analogy with the ring modulator using Schottky diodes[23]. The device consists of four nominally identical Josephson junctions forming a ring threaded by a magnetic flux Φ. This magnetic flux induces a fixed, circulating current around the ring. When operated with a bias current lower than their critical current I_0, Josephson junctions behave as pure nonlinear inductors with inductance $L_J = \varphi_0/(I_0\cos\delta)$, where δ is the gauge-invariant phase of the junction and $\varphi_0 = \hbar/2e$ is the reduced flux quantum. They

[1]Department of Physics and Applied Physics, Yale University, New Haven, Connecticut 06520-8284, USA, [2]Department of Physics, University of California, Berkeley, California 94720-7300, USA. *e-mail: michel.devoret@yale.edu.

are the only known nonlinear and non-dissipative circuit elements working at microwave frequencies. The ring has three orthogonal electrical modes coupled to the junctions: two differential ones, X and Y, and a common one, Z (Fig. 1a). They provide the minimum number of modes for three-wave mixing.

We introduce the node flux $\Phi_{i=1,\ldots,4}$ defined by

$$V_{i=1,\ldots,4} = \frac{\mathrm{d}\Phi_{i=1,\ldots,4}}{\mathrm{d}t}$$

where $V_{i=1,\ldots,4}$ are the potentials at ring nodes 1, 2, 3 and 4, and where $\mathrm{d}/\mathrm{d}t$ is the time derivative. The amplitudes of the three modes X, Y and Z can be chosen as the following combination of node fluxes:

$$\Phi_X = \Phi_1 - \Phi_2; \quad \Phi_Y = \Phi_4 - \Phi_3; \quad \Phi_Z = \Phi_1 + \Phi_2 - \Phi_3 - \Phi_4$$

In the case of large-area junctions, the charging energy owing to the intrinsic capacitance of the junctions can be ignored. Hence, the Hamiltonian of the ring is given only by the sum of the Josephson Hamiltonian of each junction $H_J = -E_J \cos\delta_{i=a,b,c,d}$, where $E_J = I_0\varphi_0$ (ref. 24). By rewriting the sum of the Josephson energies as a function of the variables Φ_X, Φ_Y and Φ_Z,

$$H_{\mathrm{ring}} = -4E_J\left[\cos\frac{\Phi_X}{2\varphi_0}\cos\frac{\Phi_Y}{2\varphi_0}\cos\frac{\Phi_Z}{2\varphi_0}\cos\frac{\Phi}{4\varphi_0} + \sin\frac{\Phi_X}{2\varphi_0}\sin\frac{\Phi_Y}{2\varphi_0}\sin\frac{\Phi_Z}{2\varphi_0}\sin\frac{\Phi}{4\varphi_0}\right] \quad (2)$$

In Fig. 1b we plot the energy of local equilibrium states of the Josephson ring modulator as a function of the magnetic flux Φ when no external currents are applied to the ring. There are four stable states satisfying the quantization of the flux through the loop. Although each state is $4\Phi_0$-periodic as a function of the flux, the envelope of the lowest-energy state remains Φ_0-periodic as required by gauge invariance ($\Phi_0 = 2\pi\varphi_0$).

Let us now consider the degenerate ground state at $\Phi = \Phi_0/2$ labelled a in Fig. 1b. For mode intensities Φ_X, Φ_Y and Φ_Z much smaller than Φ_0, we can ignore terms of order higher than three and equation (2) reduces to

$$H_{\mathrm{ring}} = \lambda\Phi_X\Phi_Y\Phi_Z + \mu[\Phi_X{}^2 + \Phi_Y{}^2 + \Phi_Z{}^2] \quad (3)$$

with $\lambda = -2\sqrt{2}\pi^3 E_J/\Phi_0{}^3$ and $\mu = \sqrt{2}\pi^2 E_J/\Phi_0{}^2$ at $\Phi = \Phi_0/2$. Apart from the sought-after pure nonlinear coupling term $\Phi_X\Phi_Y\Phi_Z$, the Hamiltonian contains a contamination term, which is only quadratic in the fluxes and which therefore renormalizes only the mode frequencies. This powerful result shows that the Josephson ring modulator can carry out the operation of mixing three orthogonal field modes while producing a minimal number of spurious nonlinear effects. The Wheatstone-bridge type of symmetry eliminates most of the unwanted terms in the Hamiltonian, in particular those of the form $\Phi_X{}^2\Phi_Z$, $\Phi_Y{}^2\Phi_Z$, $\Phi_X{}^2\Phi_Y$, $\Phi_Y{}^2\Phi_X$, which would induce other, unwanted types of mixing (see below). Note that, although $\Phi = \Phi_0/2$ is optimal for maximizing λ while keeping the working point stable, it is not a stringent condition. In the following, the differential modes X and Y are used to carry the signal and the idler with symmetric roles and the Z mode is used as the pump.

The Josephson parametric converter

We now feed the X and Y modes of the Josephson ring modulator through two superconducting resonators. A lumped-element representation of the circuit that we have named the Josephson parametric converter (JPC) is shown in Fig. 2a,b. The device contains only purely dispersive elements: superconducting

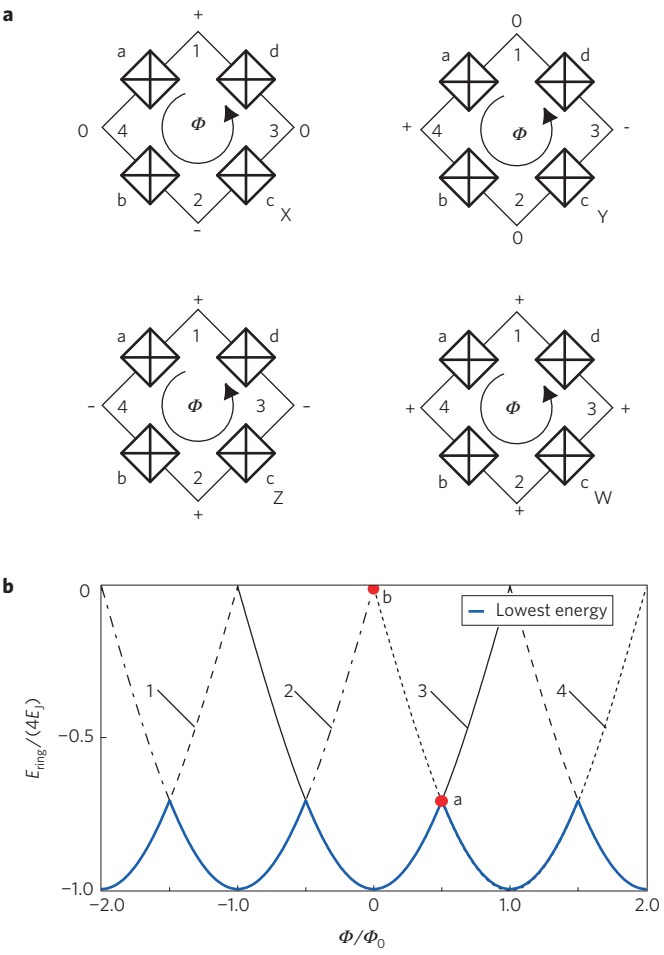

Figure 1 | Electrical modes and energy states of the Josephson ring modulator. a, The Josephson ring modulator consists of four nominally identical Josephson junctions (a, b, c and d) and has four orthogonal electrical modes. The two differential modes X, Y and the common mode Z are coupled to the junctions, whereas the fourth mode W remains uncoupled. **b**, Energy states of the ring modulator. There are four stable states satisfying the relation $\delta_a + \delta_b + \delta_c + \delta_d \bmod 2\pi = 2\pi\Phi/\Phi_0$, where δ_i is the gauge-invariant phase of junction i and where Φ_0 is the flux quantum. Each state is $4\Phi_0$ periodic as a function of the flux Φ through the loop, but the envelope (blue line) of the lowest energy remains Φ_0-periodic. Other energy extremum states are not represented here. At point a, the device can produce a pure nonlinear coupling term $\Phi_X\Phi_Y\Phi_Z$, whose contamination is only of the type $\Phi_X{}^2 + \Phi_Y{}^2 + \Phi_Z{}^2$. Point a actually corresponds to two degenerate states separated by an energy barrier whose height is $2(\sqrt{2}-1)E_J$. At point b, there is no contamination and the nonlinearity is of the purest form, but it would be very difficult to stabilize the device in an excited state.

resonators and Josephson junctions. As it has no internal dissipation, all the noise appearing at the output ports originates from the coupling of the JPC to the external circuits connected at its different ports. There are in fact two possible variations of the circuit depending on whether the ring modulator junctions are in parallel with the voltage of the resonators (Fig. 2a) or in series with the current of the resonators (Fig. 2b). For simplicity and conciseness we treat here only the first case. The second case can be treated by a simple extension of the formalism we present. The Hamiltonian of the two resonators is given by[24,25]

$$H_{\mathrm{res}} = \frac{\Phi_X{}^2}{2L_a} + \frac{Q_X{}^2}{2C_a} + \frac{\Phi_Y{}^2}{2L_a} + \frac{Q_Y{}^2}{2C_a} + H_{\mathrm{damp}}$$

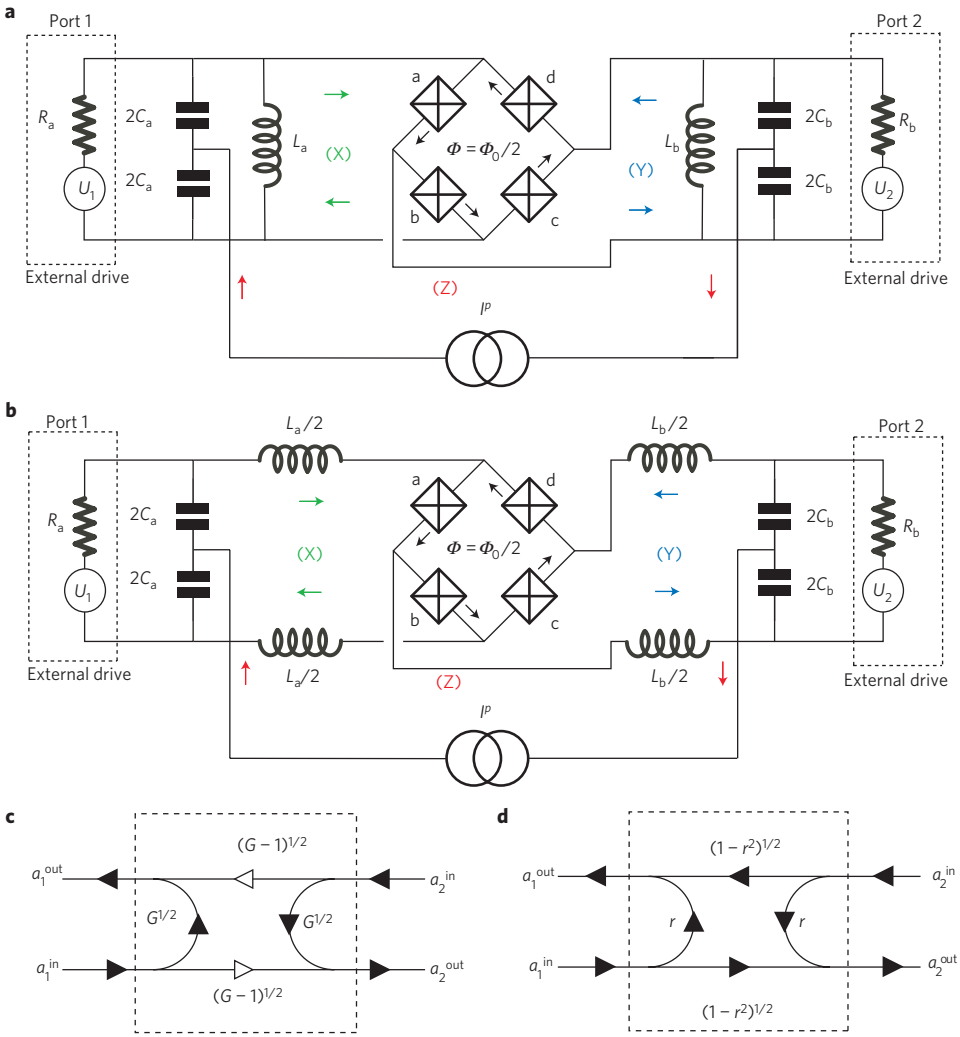

Figure 2 | Description of the Josephson parametric converter. a, Lumped-element schematic of the parallel JPC. The device is based on a ring modulator coupled to two parallel *LC* resonators corresponding to the two differential modes X and Y. The common mode Z is driven by a current source I^p. Both resonators are coupled to external drives. **b**, Lumped-element schematic of the series JPC. **c**, Scattering representation of the JPC in the case of amplification operation. Here the white arrows denote the conjugation operation because the non-diagonal terms of the scattering matrix couple a^{out} to a^{*in}. **d**, Scattering representation of the JPC in the case of the pure conversion operation.

where the Φ and the Q are the conjugated fluxes and charges in the inductive and capacitive parts of the circuit, respectively, and where the L and the C are the associated inductances and capacitances. The damping term H_{damp} arising from the coupling to the external source resistors R_a and R_b could be expressed using the Caldeira–Leggett model[26], which treats dissipation in a quantum circuit, but this detailed description is not of interest here. In addition, each resonator is submitted to a weak, time-dependent external drive, which models the incoming signal (idler). This contribution can be taken into account by introducing the Hamiltonian of the drives[24]

$$H_{drive} = -\Phi_X \frac{U_1}{R_a}\cos(\omega_1 t + \phi_1) - \Phi_Y \frac{U_2}{R_b}\cos(\omega_2 t + \phi_2) \qquad (4)$$

where $U_{1,2}$ are the amplitudes of the external voltage sources with internal resistors $R_{a,b}$ (see Fig. 1), $\omega_{1,2}$ are their angular frequencies and $\phi_{1,2}$ their phases. The pump mode is assumed to be so stiffly driven that Φ_Z can be regarded as an imposed oscillating classical field, which does not suffer back-action from its coupling to the other modes.

Therefore, the total Hamiltonian of the JPC is given by

$$H_{JPC} = H_{res} + H_{ring} + H_{drive}$$

In the following, we consider the case where the pump is driven with two tones at frequencies $\Omega_\sigma = \omega_1 + \omega_2$ and $\Omega_\delta = \omega_1 - \omega_2$ (we assume $\omega_1 > \omega_2$) and corresponding current amplitudes I^p_σ and I^p_δ. Using the Hamilton equations $\dot{Q}_X = -\partial H_{JPC}/\partial \Phi_X$ and $\dot{Q}_Y = -\partial H_{JPC}/\partial \Phi_Y$, we can derive the equations of motion for the two modes X and Y

$$\ddot{\Phi}_X + \kappa_a \dot{\Phi}_X + \omega_a^2 \Phi_X + 2\Phi_Y \left[\frac{\chi_\sigma}{C_a}\cos(\Omega_\sigma t + \varphi_\sigma) + \frac{\chi_\delta}{C_a}\cos(\Omega_\delta t + \varphi_\delta)\right] = 2\epsilon_1 \cos(\omega_1 t + \phi_1)$$

$$\ddot{\Phi}_Y + \kappa_b \dot{\Phi}_Y + \omega_b^2 \Phi_Y + 2\Phi_X \left[\frac{\chi_\sigma}{C_b}\cos(\Omega_\sigma t + \varphi_\sigma) + \frac{\chi_\delta}{C_b}\cos(\Omega_\delta t + \varphi_\delta)\right] = 2\epsilon_2 \cos(\omega_2 t + \phi_2)$$

where $\chi_\sigma = I^p_\sigma/(4\varphi_0)$ and $\chi_\delta = I^p_\delta/(4\varphi_0)$. The symbols φ_σ and φ_δ denote the initial phases of the pump drives. The coefficients $\kappa_{a(b)} = (R_{a(b)}C_{a(b)})^{-1}$ are the usual damping factors in *RLC* circuits,

$\omega_{a(b)} = \sqrt{L_{a(b)} + L_J / L_J L_{a(b)} C_{a(b)}}$ are the resonance frequencies of resonators renormalized by the quadratic terms in equation (3) and $\epsilon_{1(2)} = U_{1(2)} \kappa_{a(b)}$. Note that the presence of higher-order spurious terms would make the resonance frequencies dependent on pump power and induce instabilities. Our circuit has a direct mechanical analogue consisting of two coupled harmonic oscillators whose mutual coupling is parametrically driven. Following the usual treatment of a parametric amplifier, we impose the resonant tuning $\omega_1 = \omega_a$ and $\omega_2 = \omega_b$ and look for solutions of the form $\Phi_X = x e^{i\omega_1 t} + \text{c.c.}$ and $\Phi_Y = y e^{i\omega_2 t} + \text{c.c.}$ where c.c. is the conjugated complex. Keeping only the terms oscillating at ω_1 and ω_2, we obtain the phasors

$$x = \frac{-i\kappa_b \omega_2 \tilde{\epsilon}_1 - \frac{\tilde{\chi}_\sigma}{C_a} \tilde{\epsilon}_2^* + \frac{\tilde{\chi}_\delta}{C_a} \tilde{\epsilon}_2}{\kappa_a \kappa_b \omega_1 \omega_2 - \frac{\chi_\sigma^2}{C_a C_b} + \frac{\chi_\delta^2}{C_a C_b}} \tag{5}$$

$$y = \frac{-i\kappa_a \omega_1 \tilde{\epsilon}_2 - \frac{\tilde{\chi}_\sigma}{C_b} \tilde{\epsilon}_1^* + \frac{\tilde{\chi}_\delta^*}{C_b} \tilde{\epsilon}_1}{\kappa_a \kappa_b \omega_1 \omega_2 - \frac{\chi_\sigma^2}{C_a C_b} + \frac{\chi_\delta^2}{C_a C_b}} \tag{6}$$

where $\tilde{\chi}_\delta = \chi_\delta e^{i\varphi_\delta}$, $\tilde{\chi}_\sigma = \chi_\sigma e^{i\varphi_\sigma}$ and $\tilde{\epsilon}_1 = \epsilon_1 e^{i\phi_1}$, $\tilde{\epsilon}_2 = \epsilon_2 e^{i\phi_2}$.

From the point of view of microwave circuits, rather than the local fluxes Φ_X and Φ_Y and voltages U_1 and U_2, it is more convenient to introduce the normalized amplitudes of the incoming and outgoing modes $a_{1(2)}^{in}$ and $a_{1(2)}^{out}$ at ports 1 and 2. This transformation is described in detail in the Methods section. As a result, we can express equations (5) and (6) in a very concise way by introducing the scattering matrix S_{JPC} of the JPC.

$$\begin{pmatrix} a_1{}^{out}[\omega_1] \\ a_1{}^{*out}[-\omega_1] \\ a_2{}^{out}[\omega_2] \\ a_2{}^{*out}[-\omega_2] \end{pmatrix} = \begin{pmatrix} r_1 & 0 & t_1 & s_1 \\ 0 & r_1 & s_1^* & t_1^* \\ t_2 & s_2 & r_2 & 0 \\ s_2^* & t_2^* & 0 & r_2 \end{pmatrix} \cdot \begin{pmatrix} a_1{}^{in}[\omega_1] \\ a_1{}^{*in}[-\omega_1] \\ a_2{}^{in}[\omega_2] \\ a_2{}^{*in}[-\omega_2] \end{pmatrix}$$

where the coefficients are given, at the resonant tuning, by $r_1 = r_2 = r = (1 - |\rho_\delta|^2 + |\rho_\sigma|^2)/(1 + |\rho_\delta|^2 - |\rho_\sigma|^2)$, $t_1 = t_2^* = t = 2i\rho_\delta / (1 + |\rho_\delta|^2 - |\rho_\sigma|^2)$ and $s_2 = s_1 = s = -2i\rho_\sigma / (1 + |\rho_\delta|^2 - |\rho_\sigma|^2)$ and where we have introduced the reduced pump currents $\rho_\delta = \tilde{\chi}_\delta / \sqrt{C_a C_b \kappa_a \kappa_b \omega_1 \omega_2}$ and $\rho_\sigma = \tilde{\chi}_\sigma / \sqrt{C_a C_b \kappa_a \kappa_b \omega_1 \omega_2}$. The three coefficients r, t and s satisfy the relation $|r|^2 + |t|^2 - |s|^2 = 1$. The form of this scattering matrix is in fact rather remarkable. As we show in the Methods section, S_{JPC} has the exact minimal form required to carry out phase-preserving amplification with minimum added noise and noiseless frequency conversion. This is the consequence of (1) the dispersive nature of the operation of the device and (2) the number of modes having been kept minimal. The same matrix form is obtained with the series circuit of Fig. 2b, albeit with different expressions for the ρ.

The case $\rho_\delta = 0$ corresponds to the optimal amplification operation described in Fig. 2c. The coefficients $|r|$ and $|s|$ can then be written as $|r| = \sqrt{G} = (1 + |\rho_\sigma|^2)/(1 - |\rho_\sigma|^2)$ and $|s| = \sqrt{G - 1} = 2|\rho_\sigma|/(1 - |\rho_\sigma|^2)$. Amplification ($G \gg 1$) is obtained when the reduced pump current ρ_σ approaches unity from below. The diagonal term r can be seen as a photon 'cis-gain' characteristic of one-port reflection amplifier operation. From the point of view of each port separately, the device behaves as a sort of ideal negative resistance: the incoming wave at either port is reflected with a power gain G and its phase is preserved, when the signal at the other port is zero. A circulator is needed to separate the outgoing wave from the incoming one. The non-diagonal term s can be seen as a photon 'trans-gain' between different ports. As it couples conjugated-mode amplitudes $a_{1(2)}^{out}$ and $a_{2(1)}^{*in}$, the device behaves as a phase-conjugating frequency converter with power gain $G - 1$ (ref. 6). In particular, this operation can be used to mix down a signal from high frequency ω_1 to low frequency ω_2. The remarkable feature here is the presence of photon gain. Superconductor–insulator–superconductor mixers using the quasiparticle branch of a tunnel junction are so far the only known practical examples of mixers with gain, and they can operate fairly close to the quantum limit[27].

The case $\rho_\sigma = 0$ corresponds to a conversion mode where an incoming mode at one port is partially reflected and partially converted into the second mode (Fig. 2d). This operation is analogous to that carried out by a beam splitter but with the peculiarity that the frequency of the transmitted signal is converted when modes 1 and 2 have different frequencies ω_1 and ω_2. The device conserves the total number of incoming photons ($|r|^2 + |t|^2 = 1$), whereas the energy is conserved only if $\omega_1 = \omega_2$. Pure frequency conversion with unit gain can be obtained when $|\rho_\delta| = 1$. Although both modes of operation make frequency conversion possible, there are some fundamental differences between the two processes. The pure converter case enables us to convert frequency with no added noise and without any reflection. On the other hand, the phase-conjugating conversion of the amplification mode has the advantage of enabling photon gain.

Noise of the JPC

Let us now analyse the noise properties of the JPC for the two different cases of operation. Assuming thermal equilibrium with temperature $T \ll \hbar\omega / k_B$, each port is fed at its input with half a photon of noise arising from vacuum fluctuations. Therefore, the total output noise power emitted by each port in units of photon number per mode is

$$N^{out} = \frac{1}{2}|r|^2 + \frac{1}{2}|t|^2 + \frac{1}{2}|s|^2 = \frac{1}{2}(2(|r|^2 + |t|^2) - 1)$$

In the case of amplification ($t = 0$) with large gain ($|r| \gg 1$), the noise referred back to the input is

$$N_{eff}^{in} = N^{out}/|r|^2 (\simeq N^{out}/|s|^2) = 1 + \frac{-1}{2|r|^2} \to 1$$

Although each port is fed at its input with only half a photon of noise, after amplification the total output noise at each port is equivalent to one photon at the input ($N_{eff}{}^{in} \to 1$). This is an illustration of Caves' theorem[3]: the noise added by the amplification process to the vacuum noise already present at the input port is equivalent to half a photon ($N_{add}{}^{in} \to 1/2$).

In the pure converter case ($|s| = |r| = 0, |t| = 1$), the noise referred back to the input is

$$N_{eff}{}^{in} = N^{out}/|t|^2 = \frac{2|t|^2 - 1}{2|t|^2} = \frac{1}{2}$$

In this case, the output noise is identical to the input noise (half a photon) and no noise is added during the process ($N_{add}{}^{in} = 0$). The photon-number gain is unity, despite the fact that it is possible to have power gain when the frequency is up-converted. A more general treatment of the noise is presented in the Supplementary Information.

The general case of arbitrary detuning

Detuning the signal frequencies from the resonance frequencies of the resonators ($\omega_1 \neq \omega_a$ and $\omega_2 \neq \omega_b$) complicates the expression of S_{JPC} but retains the phase-preserving quantum limited operation to be reached when $\rho_\delta = 0$ or $\rho_\sigma = 0$. Note that when signals are applied at both ports the phase preservation property is lost.

In the amplification mode of operation ($\rho_\delta = 0$), the coefficients of S_{JPC} are given by

$$r_{1,2} = -\frac{(\vartheta_{2,1} + i)(\vartheta_{1,2} + i) - |\rho_\sigma|^2}{(\vartheta_{2,1} + i)(\vartheta_{1,2} - i) - |\rho_\sigma|^2} \quad \text{and}$$

$$s_{1,2} = \frac{-2i\rho_\sigma}{(\vartheta_{2,1} + i)(\vartheta_{1,2} - i) - |\rho_\sigma|^2}$$

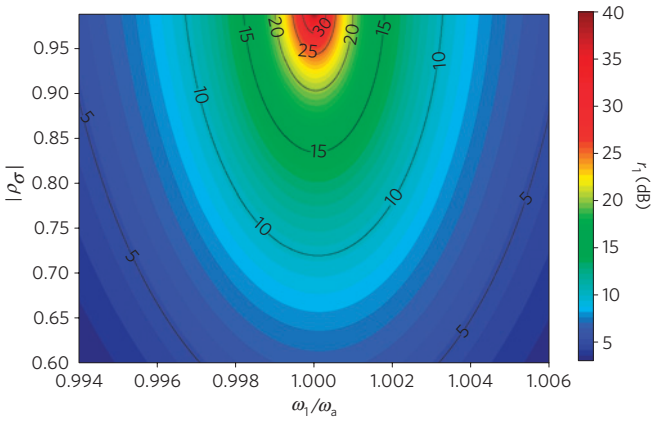

Figure 3 | Gain of the JPC. The figure shows in colour scale the gain r_1 in the amplification mode as a function of the normalized input frequency ω_1/ω_a for different values of $|\rho_\sigma|$ (from 0.6 to 0.99). In this example, $Q_a = 50$ and the damping factors are taken to be identical for the two resonators ($\omega_a/Q_a = \omega_b/Q_b$).

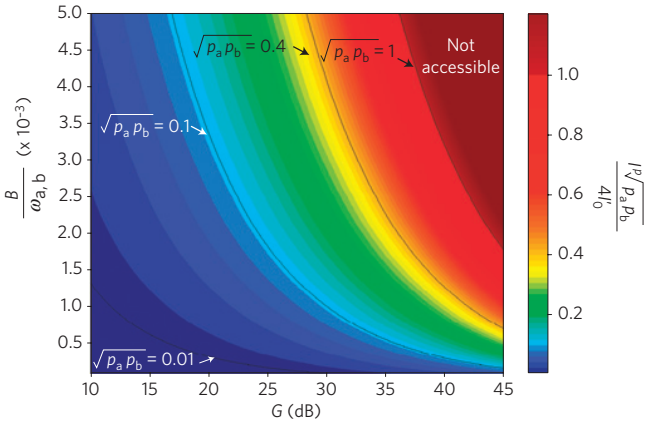

Figure 4 | Main constraint on the gain × bandwidth product of the JPC. The figure shows in colour scale the pump current in the junction, normalized by the Z-mode critical current, as a function of the relative bandwidth $B/\omega_{a,b}$ and the gain G. The corresponding brown area is not accessible for the JPC, because in this region the pump current in the junction always exceeds the critical current. The different contours correspond to the various limitations obtained for different participation ratios p_a and p_b.

where $\vartheta_1 = (\omega_1^2 - \omega_a^2)Q_a/\omega_a\omega_1$ and $\vartheta_2 = (\omega_2^2 - \omega_b^2)Q_b/\omega_b\omega_2$. Here we have introduced the quality factor of the resonators $Q_a = \omega_a/\kappa_a$ and $Q_b = \omega_b/\kappa_b$. Figure 3 shows a typical example of gain curves for different values of $|\rho_\sigma|$. In the large-gain limit the expression of $r_{1,2}$ reduces to a Lorentzian form

$$|r_{1,2}| \simeq \frac{\sqrt{G}}{\sqrt{1+G\left(\frac{Q_a}{\omega_a}+\frac{Q_b}{\omega_b}\right)^2(\omega_{1,2}-\omega_{a,b})^2}}$$

The -3 dB bandwidth of the amplifier is thus

$$B = \frac{2}{\sqrt{G}}\left(\frac{Q_a}{\omega_a}+\frac{Q_b}{\omega_b}\right)^{-1} \quad (7)$$

We arrive here at an important result: the bandwidth of the amplifier is inversely proportional to the amplitude gain $\sqrt{G}$. This feature is a general property of parametric amplifiers. At this point, we would like to stress that the 'tuning bandwidth' of the amplifier, that is, the range of frequencies over which the centre frequency of the signal bandwidth (equation (7)) can be varied, remains equal to the resonator bandwidth $\kappa_{a,b}$. Here, detuning the pump frequency Ω_σ away from the resonance condition $\Omega_\sigma = \omega_a + \omega_b$ displaces the centres of the signal and idler bandwidth inside the larger bandwidth of the resonators. The case of an arbitrary detuning for the conversion mode of operation is treated in the Methods section.

Practical issues: Gain, bandwidth, dynamic range and stability

We now analyse some practical issues and show that we can build a practical device that would be useful for many different applications. The questions of power gain and bandwidth are central and are intimately related. Ideally, the amplified noise should be much larger than the noise of the following amplifier in the measurement chain. For a quantum-limited amplifier working at gigahertz frequencies and assuming the best state-of-the-art commercial device as a following amplifier (a noise temperature of a few Kelvin is typical), the power gain has to be at least 20 dB, although of course a smaller power gain can still lead to an improvement in the overall system noise temperature. To optimize the ability of the amplifier to follow fast signals, a bandwidth around the carrier frequency that is as large as possible is sought. However, as shown by relation equation (7), the parametric coupling imposes that the signal bandwidth decreases with the amplitude gain. Although the gain of the JPC should in principle reach any arbitrarily large value when $|\rho_\sigma|$ approaches unity sufficiently closely, two limitations can occur. The first limitation is that when $|\rho_\sigma| \to 1^-$ the fraction of the pump current feeding the junctions should remain well below the Z-mode critical current $I'_0 = I_0\cos\Phi/4\varphi_0 = I_0/\sqrt{2}$ for the parametric amplification to remain stable (higher-order nonlinear terms invade the behaviour of the device as the critical current is reached). It is useful to rewrite the expression of $|\rho_\sigma|$ as

$$|\rho_\sigma| = \frac{1}{4}\sqrt{Q_aQ_bp_ap_b}\frac{I_\sigma^p}{I'_0}$$

in which we introduce the participation ratios of the inductance of the Josephson ring modulator to the resonators' inductance $p_{a,b} = L_{a,b}/(L_J + L_{a,b})$ in the parallel case and $p_{a,b} = L_J/(L_J + L_{a,b})$ in the series case. As each junction receives a quarter of the total pump current, the first limitation thus translates into

$$\sqrt{Q_aQ_bp_ap_b} > 1 \quad (8)$$

Figure 4 shows the constraints on the JPC bandwidth and gain G imposed by this limitation. This figure illustrates the impossibility of obtaining at the same time a high gain value and a large bandwidth with a parametric amplifier. Although this figure would seem to suggest that the participation ratios p_a and p_b should be as high as possible, in practice dynamic range considerations limit this possibility (see below). The second limitation arises from the fact that the sum of the resonator energies, each being weighted by its participation ratio, cannot exceed the Josephson energy. We write this new condition as

$$E_ap_a + E_bp_b < E_J$$

In particular, the amplified zero-point quantum noise cannot exceed the Josephson energy

$$G\hbar(p_a\omega_a + p_b\omega_b)/2 < E_J \quad (9)$$

Taking $p_a = p_b = p$ to simplify the algebra, we can rewrite equation (9) as

$$G < \frac{Z_Q}{Z_c} p^{0,-2} \quad (10)$$

where $Z_Q = \varphi_0^2/\hbar = \hbar/(2e)^2 \simeq 1\,\mathrm{k}\Omega$ is the quantum of impedance and $Z_c = \omega_a + \omega_b/\sqrt{C_a C_b}\omega_a\omega_b$ is an impedance characterizing the resonators. Using a conventional microwave technology, this impedance would be of the order of 50 Ω. The exponents 0 and −2 refer to the parallel and series cases respectively.

The power-gain × bandwidth product is an important characteristic, which determines the total flow of information that can be processed by the amplifier. Equations (7), (8) and (10) can be combined to obtain an important bound on this product

$$G \times B = \frac{\omega}{Q} G^{1/2} < \omega \sqrt{\frac{Z_Q}{Z_c}} p^{+1,0}$$

where we have taken $\omega_a = \omega_b = \omega$ and $Q_a = Q_b = Q$ to simplify the algebra. As $p < 1$, the final upper bound on the gain × bandwidth product is thus $G \times B < \omega\sqrt{Z_Q/Z_c}$. Thus, both parallel and series circuits have the same limitation on the power-gain × bandwidth product. However, in the case of the parallel circuit the maximum gain is strongly constrained by relation (10). Therefore, the series case seems more favourable in most practical cases. Another important characteristic of an amplifier is its dynamic range, that is, for a given gain, the maximum input power P_{max} that the device can amplify before it starts to saturate. The same considerations involving the maximum power produced by the device, as developed in relation (9), can be used to obtain the dynamic range.

$$2Gp\left(\frac{P_{max}}{B} + \frac{\hbar\omega}{2}\right) < E_J$$

Therefore

$$P_{max} < \frac{B}{2}\left(\frac{E_J}{Gp} - \hbar\omega\right)$$

However, when the input power becomes too large, our small-amplitude approximation is no longer valid and higher nonlinear terms in equation (2) start to play a part. Therefore, experimentally, the amplifier may saturate before reaching the theoretical value.

We now turn to the question of stability. The point $\rho_\sigma = 1$ corresponds to the onset of spontaneous self-oscillations of the system. Therefore, the JPC should be operated at a distance from this critical point that is safe with regard to fluctuations in pump drive power. However, the situation is better controlled here than in previous studies, where optimization of gain would conflict with increased noise caused by proximity to a poorly identified instability[28–30], whose influence might be difficult to avoid.

Production of entangled signal pairs and dynamic cooling

The gain of the JPC is high enough to potentially raise the level of quantum fluctuations much higher than the level of the noise of the second amplifier in the chain. An interesting experiment consists of turning on the pump without feeding in any signals at the input ports of the JPC. Quantum mechanically, the pump can still produce output signals, which can be seen as arising from the amplification of zero-point motion fluctuations. Moreover, as the scattering matrix conserves the volume of the phase space, the amplified noise appearing at the two ports must be entirely correlated. The function that is carried out is two-mode squeezing[31]. As the output signals can have many real microwave photons, such a device could be used for analog quantum encryption[32].

Another interesting feature of the pure frequency-converter mode of operation is that, unlike the amplifier mode, it has no added noise at the output. The JPC device operating in this case with a unit-photon-number 'trans-gain' can swap the photons at the two ports and be used as a refrigerator. Suppose that the frequency at port 2 is much smaller than the frequency at port 1, which sees an environment cold in the sense $\hbar\omega_1 \gg k_B T_1$. Initially port 2 is seeing an environment that is hot in the sense $\hbar\omega_2 \ll k_B T_2$. When the JPC is operated, the photons at port 2 are shuttled to port 1, where they are evacuated, whereas zero-point photons from port 1 go in the other direction to replace the photons at port 2, imposing vanishing temperature. The cooling rate being $\dot{q} = k_B T_2 \kappa_b$, the refrigeration power is only of the order of 1 pW at 4 K and for a bandwidth of 1 GHz, but it can be very useful for a high-Q resonator isolated from the thermal bath.

Conclusion

The Josephson parametric converter would fill a niche that has up to now been unavailable in the landscape of microwave processing devices, that of three-wave mixing for non-degenerate parametric amplification operating at the quantum limit. Moreover, we would like to stress that the present level of control in the dynamics of tunnel junctions in resonant circuits, as demonstrated by recent several successful operations[13–15,33,34], ensures that its realization is entirely within reach. This development would bring the subject of analog radio-frequency quantum signal processing (should we nickname it quantum radioelectricity?) to a qualitatively new level.

Methods

Transformation of local fluxes and voltages to travelling waves. In the circuit of Fig. 2a, the local fluxes and voltages can be expressed as a function of the amplitudes of the incoming and outgoing modes A^{in} and A^{out} at ports 1 and 2 using the following relations:

$$A_1^{in} + A_1^{out} = \frac{V_1 - V_2}{\sqrt{R_a}} = \frac{i\omega_1 x}{\sqrt{R_a}}; \quad A_2^{in} + A_2^{out} = \frac{V_4 - V_3}{\sqrt{R_b}} = \frac{i\omega_2 y}{\sqrt{R_b}};$$

$$A_1^{in} = \frac{U_1}{2\sqrt{R_a}}; \quad A_2^{in} = \frac{U_2}{2\sqrt{R_b}}$$

A^{in} and A^{out} are expressed in the square root of watts. We can now define the normalized amplitude a^{in} and a^{out} expressed in the square root of photon number per unit time.

$$a_1^{in} = \frac{A_1^{in}}{\sqrt{\hbar\omega_1}}; \quad a_2^{in} = \frac{A_2^{in}}{\sqrt{\hbar\omega_2}}; \quad a_1^{out} = \frac{A_1^{out}}{\sqrt{\hbar\omega_1}}; \quad a_2^{out} = \frac{A_2^{out}}{\sqrt{\hbar\omega_2}}$$

At this point, the normalized amplitudes are still classical variables. The passage to the creation and annihilation operators is carried out by the simple replacement $a \to \hat{a}$ and $a^* \to \hat{a}^\dagger$.

Minimal scattering matrix for quantum information processing. To carry out information processing at the quantum limit, a device must fulfil requirements that impose a constraint on its scattering matrix S. In this section we derive the minimal form of S that achieves phase-preserving amplification with minimal added noise and noiseless frequency conversion in the case of a device involving only two modes. Following a route similar but not identical to that pioneered by Caves, we introduce the generalized scattering matrix S of a linear microwave device, which relates input and output modes at its different ports.

$$\Lambda^{out} = S \cdot \Lambda^{in}$$

Here we have introduced the mode-amplitude input and output vectors

$$\Lambda^{in} = \begin{pmatrix} a_1^{in} \\ a_1^{*in} \\ \vdots \\ a_n^{in} \\ a_n^{*in} \end{pmatrix}; \quad \Lambda^{out} = \begin{pmatrix} a_1^{out} \\ a_1^{*out} \\ \vdots \\ a_n^{out} \\ a_n^{*out} \end{pmatrix}$$

where the symbol * denotes complex conjugation. The a_n are normalized mode amplitudes expressed in the square root of photon number per unit time. Although they are at first treated as classical scalar fields, they can, in a later quantum mechanical treatment, be formally replaced by annihilation ($a_n \to \hat{a}_n$) and creation ($a_n^* \to \hat{a}_n^\dagger$) operators. Both a and a^* have to be present in the input and output

vectors because of possible phase-conjugating processes coupling an a^{out} to an $a^{*\mathrm{in}}$. In the case of a device with two ports, the most general matrix has only eight independent complex coefficients.

$$S=\begin{pmatrix} r_1 & u_1 & t_1 & s_1 \\ u_1^* & r_1^* & s_1^* & t_1^* \\ t_2 & s_2 & r_2 & u_2 \\ s_2^* & t_2^* & u_2^* & r_2^* \end{pmatrix}$$

Our requirement of information processing at the quantum limit implies that the scattering matrix must describe a canonical transformation that preserves the commutation relations of the bosonic fields $[\hat{a}_n^{\mathrm{out}},\hat{a}_n^{\dagger\mathrm{out}}]=[\hat{a}_n^{\mathrm{in}},\hat{a}_n^{\dagger\mathrm{in}}]$. Mathematically, this is translated by the property of symplecticity of the S matrix[35]

$$^{T}SJS=J$$

where

$$J=\begin{pmatrix} 0 & 1 & 0 & 0 \\ -1 & 0 & 0 & 0 \\ 0 & 0 & 0 & 1 \\ 0 & 0 & -1 & 0 \end{pmatrix}$$

To carry out phase-preserving amplification, we need to impose that the reflection at each port separately preserves the phase of the signal (that is, a phase shift of the incoming wave results in an identical phase shift of the outgoing wave). That implies that $u_1=u_1^*=u_2=u_2^*=0$. Finally, for simplicity and because it corresponds to the case of the JPC, we impose the modulus of the reflection coefficients to be identical at each port ($|r_1|=|r_2|=|r|$). However, the general case would not introduce new meaningful features and could be treated by a simple extension of the present treatment. It follows that S has the minimal form

$$S=\begin{pmatrix} |r|\mathrm{e}^{\mathrm{i}\alpha_1} & 0 & |t|\mathrm{e}^{\mathrm{i}\beta_1} & |s|\mathrm{e}^{\mathrm{i}\gamma_1} \\ 0 & |r|\mathrm{e}^{-\mathrm{i}\alpha_1} & |s|\mathrm{e}^{-\mathrm{i}\gamma_1} & |t|\mathrm{e}^{-\mathrm{i}\beta_1} \\ -|t|\mathrm{e}^{\mathrm{i}(\alpha_1+\alpha_2-\beta_1)} & |s|\mathrm{e}^{\mathrm{i}(\alpha_2-\alpha_1+\gamma_1)} & |r|\mathrm{e}^{\mathrm{i}\alpha_2} & 0 \\ |s|\mathrm{e}^{-\mathrm{i}(\alpha_2-\alpha_1+\gamma_1)} & -|t|\mathrm{e}^{-\mathrm{i}(\alpha_1+\alpha_2-\beta_1)} & 0 & |r|\mathrm{e}^{-\mathrm{i}\alpha_2} \end{pmatrix}$$

where the coefficients are linked by the relation $|r|^2+|t|^2-|s|^2=1$.

The case $s=0$ corresponds to a conversion operation where an incoming mode at one port is partially reflected and partially converted into the second mode. As $|r|^2+|t|^2=1$, the total number of photons is conserved during the process. The case $t=0$ corresponds to an amplification operation because the total number of photons is no longer conserved ($|r|^2+|s|^2\neq 1$). Therefore, $|r|$ can take any value larger than one, the phase of the signal being preserved. This matrix has the simplest form for carrying out phase-preserving amplification and frequency conversion at the quantum limit.

Case of arbitrary detuning for the conversion mode of operation. In the conversion mode of operation ($\rho_\sigma=0$)

$$r_{1,2}=-\frac{(\vartheta_{2,1}-i)(\vartheta_{1,2}+i)-|\rho_\delta|^2}{(\vartheta_{2,1}-i)(\vartheta_{1,2}-i)-|\rho_\delta|^2} \quad \text{and}$$

$$t_{1,2}=\frac{-2i\rho_\delta}{(\vartheta_{2,1}-i)(\vartheta_{1,2}-i)-|\rho_\delta|^2}$$

where $\vartheta_1=(\omega_1^2-\omega_a 2)Q_a/\omega_a\omega_1$ and $\vartheta_2=(\omega_2^2-\omega_b^2)Q_b/\omega_b\omega_2$.

Received 31 July 2009; accepted 22 December 2009; published online 14 February 2010

References

1. Shimoda, K., Takahasi, H. & Townes, C. H. Fluctuations in amplification of quanta with application to Maser amplifiers. *J. Phys. Soc. Jpn* **12,** 686–700 (1957).
2. Haus, H. A. & Mullen, J. A. Quantum noise in linear amplifiers. *Phys. Rev.* **128,** 2407–2413 (1962).
3. Caves, C. M. Quantum limits on noise in linear amplifiers. *Phys. Rev. D* **26,** 1817–1839 (1982).
4. Tien, P. K. Parametric amplification and frequency mixing in propagating circuits. *J. Appl. Phys.* **29,** 1347–1357 (1958).
5. Louisell, W. H. *Coupled Mode and Parametric Electronics* (John Wiley, 1960).
6. Louisell, W. H., Yariv, A. & Siegman, A. E. Quantum fluctuations and noise in parametric processes. I. *Phys. Rev.* **124,** 1646–1654 (1961).
7. Gordon, J. P., Louisell, W. H. & Walker, L. R. Quantum fluctuations and noise in parametric processes. II. *Phys. Rev.* **129,** 481–485 (1963).
8. André, M.-O., Mück, M., Clarke, J., Gail, J. & Heiden, C. Radio-frequency amplifier with tenth-kelvin noise temperature based on a microstrip direct current. *Appl. Phys. Lett.* **75,** 698–700 (1999).
9. Spietz, L., Irwin, K. & Aumentado, J. Input impedance and gain of a gigahertz amplifier using a dc superconducting quantum interference device in a quarter wave resonator. *Appl. Phys. Lett.* **93,** 082506 (2008).
10. Yurke, B. *et al.* Observation of parametric amplification and deamplification in a Josephson parametric amplifier. *Phys. Rev. A* **39,** 2519–2533 (1989).
11. Yurke, B. Observation of 4.2-K equilibrium-noise squeezing via a Josephson-parametric amplifier. *Phys. Rev. Lett.* **60,** 764–767 (1988).
12. Movshovich, R. *et al.* Observation of zero-point noise squeezing via a Josephson-parametric amplifier. *Phys. Rev. Lett.* **65,** 1419–1422 (1990).
13. Wallraff, A. *et al.* Strong coupling of a single photon to a superconducting qubit using circuit quantum electrodynamics. *Nature* **431,** 162–167 (2004).
14. Lupaşcu, A. *et al.* Quantum non-demolition measurement of a superconducting two-level system. *Nature Phys.* **3,** 119–125 (2007).
15. Mika, A., Sillanpää, M. A., Park, J. I. & Simmonds, R. W. Coherent quantum state storage and transfer between two phase qubits via a resonant cavity. *Nature* **449,** 438–442 (2007).
16. Majer, J. *et al.* Coupling superconducting qubits via a cavity bus. *Nature* **449,** 443–447 (2007).
17. Castellanos-Beltran, M. A. & Lehnert, K. W. Widely tunable parametric amplifier based on a superconducting quantum interference device array resonator. *Appl. Phys. Lett.* **91,** 083509 (2007).
18. Castellanos-Beltrana, M. A., Irwin, K. D., Hilton, G. C., Vale, L. R. & Lehnert, K. W. Amplification and squeezing of quantum noise with a tunable Josephson metamaterial. *Nature Phys.* **4,** 928–931 (2008).
19. Tholeń, E. A. Nonlinearities and parametric amplification in superconducting coplanar waveguide resonators. *Appl. Phys. Lett.* **90,** 253509 (2007).
20. Yamamoto, T. *et al.* Flux-driven Josephson parametric amplifier. *Appl. Phys. Lett.* **93,** 042510 (2008).
21. Zhang, Q., Ruskov, R. & Korotkov, A. N. Continuous quantum feedback of coherent oscillations in a solid-state qubit. *Phys. Rev. B* **72,** 245322 (2005).
22. Korotkov, A. N. Simple quantum feedback of a solid-state qubit. *Phys. Rev. B* **71,** 201305 (2005).
23. Pozar, D. M. *Microwave Engineering* 629 (Wiley, 2005).
24. Devoret, M. H. *Quantum Fluctuations: Les Houches Session LXIII* (Elsevier, 1997).
25. Yurke, B. & Denker, J. S. Quantum network theory. *Phys. Rev. A* **29,** 1419–1437 (1984).
26. Caldeira, A. O. & Legget, A. J. Quantum tunneling in a dissipative system. *Ann. Phys.* **149,** 374–456 (1983).
27. Mears, C. A Quantum-limited heterodyne detection of millimetre waves using superconducting tantalum tunnel junctions. *Appl. Phys. Lett.* **57,** 2487–2489 (1990).
28. Wahlstein, S., Rudner, S. & Claeson, T. Arrays of Josephson tunnel junctions as parametric amplifiers. *J. Appl. Phys.* **49,** 4248–4263 (1979).
29. Mygind, N., Perdersen, F., Soerensen, O. H., Dueholm, B. & Levinsen, M. T. Low-noise parametric amplification at 35 GHz in a single Josephson tunnel junction. *Appl. Phys. Lett.* **35,** 91–93 (1979).
30. Bryant, P., Wiesenfeld, K. & McNamara, B. Noise rise in parametric amplifiers. *Phys. Rev. B* **36,** 752–755 (1987).
31. Bjork, G. & Yamamoto, Y. Generation of nonclassical photon states using correlated photon pairs and linear feedforward. *Phys. Rev. A* **37,** 4229–4239 (1984).
32. Grosshans, F. & Grangier, P. Continuous variable quantum cryptography using coherent states. *Phys. Rev. Lett.* **88,** 057902 (2002).
33. Siddiqi, I. *et al.* RF-driven Josephson bifurcation amplifier for quantum measurement. *Phys. Rev. Lett.* **93,** 207002 (2004).
34. Metcalfe, M. *et al.* Measuring the decoherence of a quantronium qubit with the cavity bifurcation amplifier. *Phys. Rev. B* **76,** 174516 (2007).
35. Guillemin, V. & Sternberg, S. *Symplectic Techniques in Physics* (Cambridge Univ. Press, 1984).

Acknowledgements

This work was supported by NSA through ARO grant number W911NF-05-01-0365, the Keck foundation and the NSF through grant number DMR-032-5580. M.H.D. acknowledges partial support from College de France. We are indebted to B. Abdo for help with the proof corrections.

Author contributions

M.H.D. proposed the original idea of the ring modulator. N.B. and M.H.D. developed the device, carried out the theoretical analysis and wrote the article. R.V., V.E.M. and I.S. contributed extensively to discussions of the results. S.M.G. introduced all authors to the multifunctional aspect of three-wave mixing. R.J.S. contributed by his knowledge of ultralow-noise microwave circuits and measurements.

Additional information

The authors declare no competing financial interests. Supplementary information accompanies this paper on www.nature.com/naturephysics. Reprints and permissions information is available online at http://npg.nature.com/reprintsandpermissions. Correspondence and requests for materials should be addressed to M.H.D. or N.B.